ON GRAIN BOUNDARY TOPOGRAPHY AND SURFACE REACTIVITY DURING HOT-DIP GALVANISING

Nils Köpper, Friedrich Luther and Thomas Koll
Salzgitter Mannesmann Forschung GmbH, Germany

ABSTRACT

Under certain conditions of oxygen shortage and high temperatures as could occur after coiling a hot-rolled strip, alloying elements can diffuse and oxidise preferably along grain boundaries, causing a depletion zone of solute alloying elements in the surface near region. When oxides are present along grain boundaries, pickling can alter surface topography by selective dissolution of these oxides on the µm-scale (µ-topography). This altered topography and the depletion of alloying elements influence diffusion properties during intercritical annealing prior to hot dip galvanising, leading to a reduced surface segregation of alloying elements. This effect was exemplified by pickling and subsequently cold rolling a hot rolled high strength steel strip with and without internally oxidized grain boundaries, using an adapted process. Samples with and without altered topography were galvanized in a hot-dip simulator with varying annealing parameters and subsequently characterized in terms of surface enrichment of alloying elements, inhibition layer density as well as crash relevant automotive zinc adhesion tests. Surfaces with altered µ-topography show lower surface segregation of alloying elements, can build more dense inhibition layers during hot-dip galvanising with the same annealing conditions, and exhibit improved coating adhesion. This effect could be helpful to enhance galvanisability of future challenging steel grades.

KEYWORDS

selective oxidation, hot rolled steel, inhibition layer, surface reactivity, segregation, depletion zone

INTRODUCTION

Lightweight construction is still an important factor in the development of new vehicle concepts in the automotive industry. Especially against the background of CO_2 savings, this topic is of increasing relevance. This is creating the desire for higher strength and ductile steels and is therefore an important driving force for the development of new steels. However, significant quantities of alloying elements like Mn, Si, Cr or Al are required to achieve the desired mechanical properties. These alloying elements show a high affinity to oxygen and can oxidize selectively at the steel surface by diffusion processes during recrystallization annealing prior to galvanising, impairing zinc wetting. Several methods have been developed to improve galvanisability of highly alloyed steels, like dew point control of the annealing atmosphere, oxidation/reduction treatments or even the use of various flash pre-coatings. Many studies have investigated e.g. the influence of annealing conditions during galvanising [1, 2, 3, 4]. However, during production of galvanized cold-rolled steel strips, the material undergoes a variety of rolling and heat treatment processes that can affect galvanising behaviour. This contribution deals with the influence of grain boundary oxidation in the coil after hot rolling on the galvanisability of cold rolled dual phase steels. The phenomenon of grain boundary oxidation in the coiled state was already investigated by Auinger et al. [5] and Ronquetti et al. [6], showing that low oxygen content and high coiling temperatures are appropriate for selective internal oxidation along grain boundaries.
For this study, starting material with and without oxidized grain boundaries in the coiled hot rolled strip was produced in an adapted industrial process using elevated coiling temperatures to investigate the influence of these two states on the galvanising process. Reference samples (“R”)

without oxidized grain boundaries were taken from the hot strip outer winding, as sufficient oxygen ingress and a high cooling rate can be guaranteed at this strip position. Samples with internal oxides along the grain boundaries were taken from the hot strip centre (samples with altered condition, "A"), where oxygen access is limited because of the tight windings and decreased cooling rate. Moreover, decarburization reactions consume oxygen [7, 8].

1. EXPERIMENTAL

Samples of a C1.8Mn0.3Si0.4Cr steel were taken in 2.6 mm hot rolled (scaled) as well as in 1.0 mm cold rolled condition from strip tail (outer winding, reference) and centre area (altered condition, A) of the hot strip as illustrated in Fig. 1. Hot and cold rolled samples were characterised by GDOES (Spectruma GDA 750) and SEM/EDX (Tescan, Mira 3). The cold rolled samples were cut down to specimens of 190 mm x 130 mm for annealing and hot dip galvanising trials.

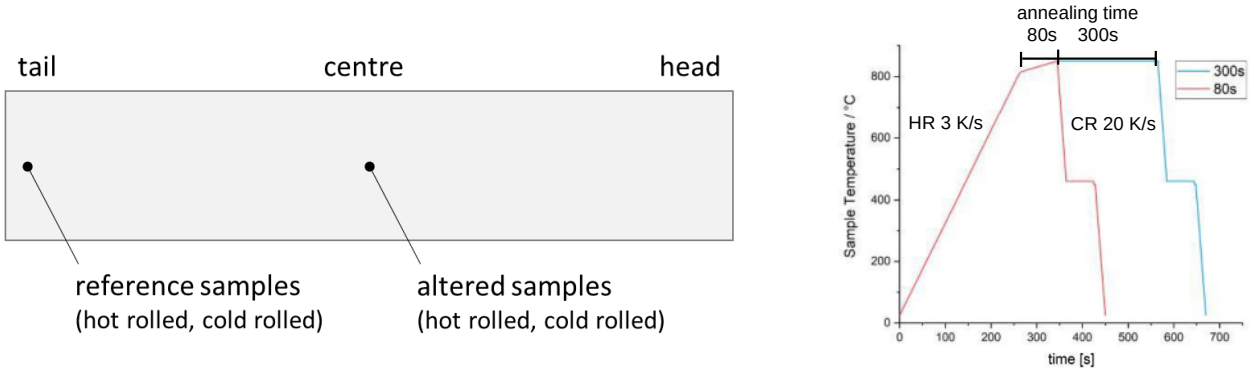

Fig. 1: Sampling positions and annealing cycles for hot dip galvanising trials.

For the annealing and galvanising experiments, the specimens were cleaned in an alkaline solution at 70 °C to remove any residual contaminants. The annealing treatment was performed in a GALVASIM hot-dip galvanising simulator in an atmosphere containing N_2-4%H_2 with dewpoints of -10 °C, -30 °C, or -50 °C, followed by 3 s hot-dipping in an Fe-saturated zinc bath containing 0.20 wt.% Al at 460 °C. The annealing time was set to 80 s and 300 s with an intercritical annealing temperature set to 850 °C as shown in the full annealing cycle in Fig. 1. The resulting zinc adhesion was tested by ball impact test based on SEP1931 and glue bead test based on BMW AA-0509, using structural adhesive BM1496V from Dow Chemicals. For assessing the inhibition layer density, the zinc coatings were selectively dissolved by a potentiostatic method using an I-Bank M Lab 500 potentiostat with a potential of 950 mV against a saturated Ag/AgCl reference electrode and finally analysed by SEM. GDOES depth profiles were made from the non-coated area of each sample in immediate vicinity of the control thermocouple. All GDOES samples were sputtered with gold before analysis to enhance the surface sensitivity of this method.

2. RESULTS AND DISCUSSION

Hot rolled state

The surface-near regions of the altered (A) and reference (R) samples differ significantly from each other, see Fig. 2. The SEM micrographs of the hot-rolled samples A show significant oxidation along grain boundaries below the scale layer. On the contrary, the reference hot-rolled sample does not show internal oxidation of alloying elements, but uniform scaling at the steel surface. It is also noticeable that condition A shows particles of reduced iron oxide on top of the scale layer. This

indicates, at least temporarily, prevailing reductive conditions for iron within the coil windings. These conditions may have been formed by the strongly limited oxygen influx into the enclosed gas volume between the coil windings in combination with high temperature and CO from decarburization reaction as reducing agent. As indicated in the EDX Mapping in Fig. 2 (left side), the regions of reduced iron oxide are large and for this reason cannot be explained by wüstite decomposition alone. Both states exhibit a Si- and Cr-rich scale layer in the interface between steel and scale.

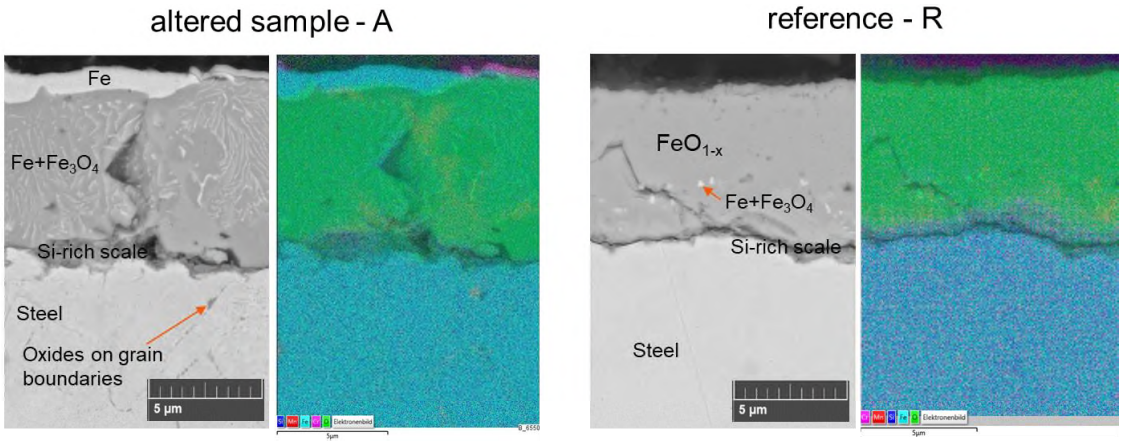

Fig. 2: SEM micrographs and EDS-Mappings of altered sample A (left) and reference (right) after hot rolling (scaled).

The GDOES depth profiles show a Mn-depletion zone in sample A as a result of the observed internal oxidation as well as a significant decarburization of about 20 µm, which is not present in the reference samples, see Fig. 3. Concerning the Si- and Cr-rich scale layer, GDOES profiles for Si und Cr show a comparable level for A und R samples, indicating that this layer has formed before coiling of the hot rolled strip, which is in line with previous investigations [9, 16].

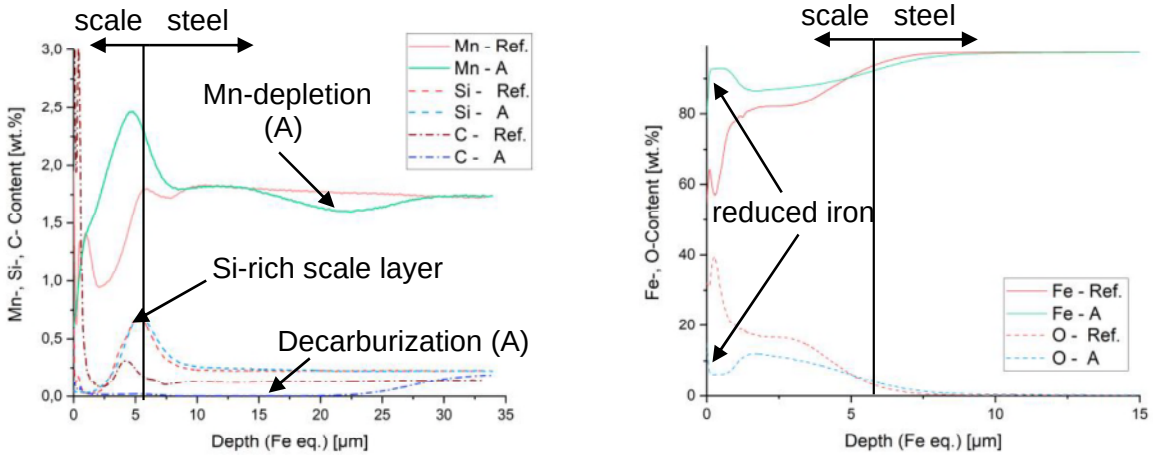

Fig. 3: GDOES depth profiles from hot rolled (scaled) altered and reference samples for Si, Mn, C (left), and Fe, O (right).

It is believed that the wüstite layer itself acts as oxygen source for internal oxidation, if the oxygen partial pressure in the enclosed atmosphere of the coil windings in the strip middle is no longer

sufficient for oxidation of iron and the driving force for further iron diffusion through the scale is missing [5, 10, 15]. However, if sufficient oxygen is present, as in the area of the outer winding, no internal oxidation takes place. In low-oxygen conditions, the diffusion depth and thus the zone of influence can be adjusted via the coiling temperature.

After pickling in hydrochloric acid with addition of an inhibitor, the surface topography of samples A is altered by selective dissolution of internal oxides along the grain boundaries on the µm-scale (µ-topography), see Fig. 4. The light optical images (LOM) from cross sections of the A samples show distinct channels along the grain boundaries, which are not present for the reference samples. In SEM top view the surfaces of the pickled A samples show a highly porous iron phase above the former steel/scale interface. This is assumed to be reduced wüstite, giving a strong indication for wüstite as oxygen source for internal oxidation of alloying elements. However, this porous layer is not present at the reference condition after pickling.

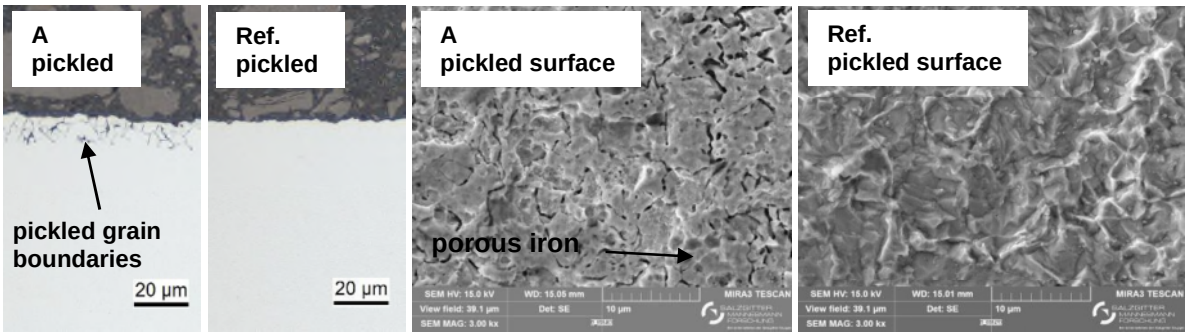

Fig. 4: LOM cross sections (left) and SEM top views (right) of altered and reference hot rolled samples after pickling with inhibitor (80 °C, 120 s).

Cold rolled state

After cold rolling prior to annealing, GDOES depth profiles of altered and reference samples show clear differences, see Fig. 5. Sample A with internal oxidation in the hot-rolled state shows a clear depletion of the alloying elements Mn and Cr near the surface down to a depth of several µm, which is a strong evidence that Mn and Cr segregated and oxidised at the grain boundaries and their oxides were subsequently removed by pickling. Silicon, on the other hand, is enriched on the direct surface in both conditions A and R, which is presumably due to residues of fayalite scale that are difficult to pickle [16].

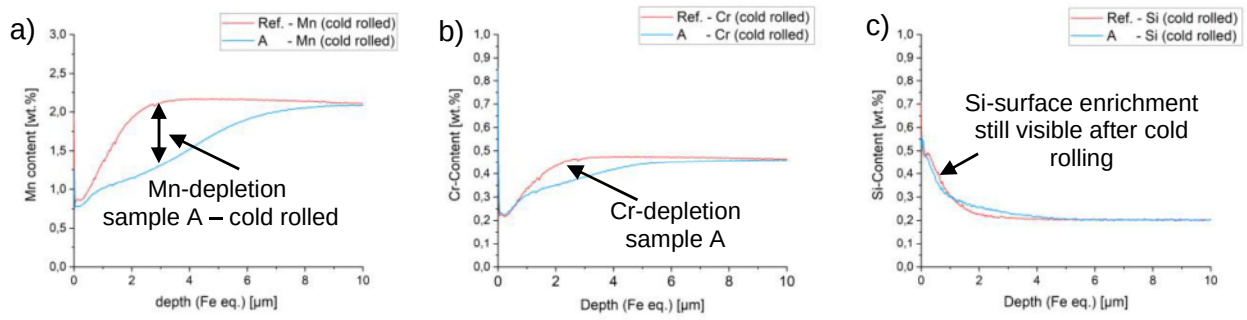

Fig. 5: GDOES depth profiles from cold rolled (CR) samples R and A for Mn (a), Cr (b) and Si (c).

In SEM top view on the cold rolled surface, clear differences are still visible between both states, as indicated in Fig. 6. The altered samples show a more pronounced structuring of the surface at µm

scale in comparison to the reference. The cross sections support this observation as only the A specimens show cleared grain boundaries below the steel surface to a depth of about 5 - 6 µm.

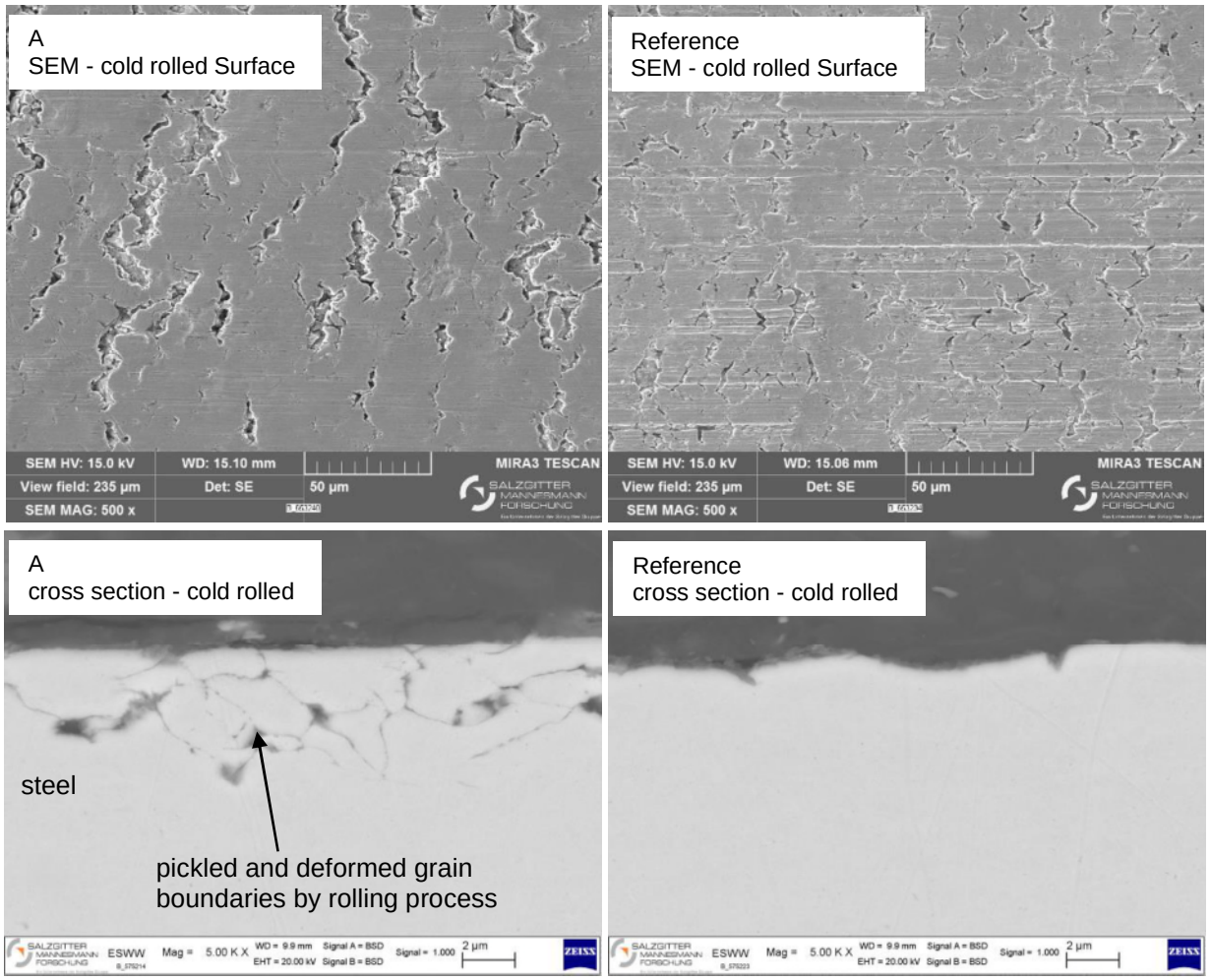

Fig. 6: SEM top views and cross sections from cold rolled samples, reference (left) and A (right).

Hot-dip galvanising experiments

After an annealing and galvanising step with varying dew points the non-coated areas of the samples show external selective oxidation of alloying elements to different extents as expected. However, there are also noticeable differences in terms of oxide formation for the same dew point between altered and reference samples, see Fig. 7.

In dry annealing gas atmosphere with long annealing cycle, both states show film-like oxide growth on the surface. At dew point -30 °C, the reference shows strongly faceted oxides covering almost the entire surface. In contrast, only a few, mainly globular lens type oxides can be observed along the grain boundaries of the annealed A sample. At dew point -10 °C, both samples show larger Mn-rich faceted oxides. The A sample additionally shows few fine globular oxides on the surface, whereas the reference sample exhibits almost complete coverage with small faceted oxides.

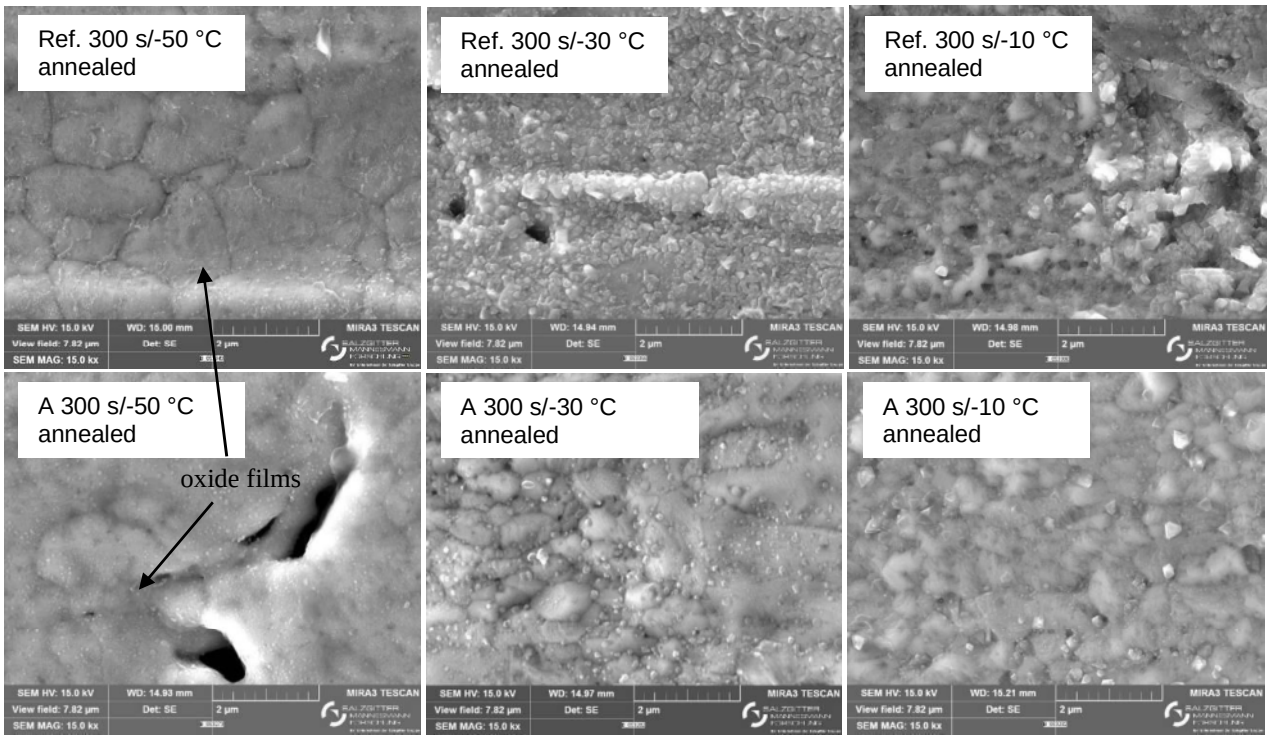

Fig. 7: SEM top views of external oxide formation on altered and reference cold rolled samples after 300 s annealing step.

The oxide morphologies with short annealing times are comparable to long annealing times at high dew points, albeit with less pronounced external oxidation. On the other hand, in dry atmosphere with dew point -50 °C a globular formation of the external oxides can be observed for A samples and in contrast a completely covering oxide film for the reference samples, see Fig. 8.

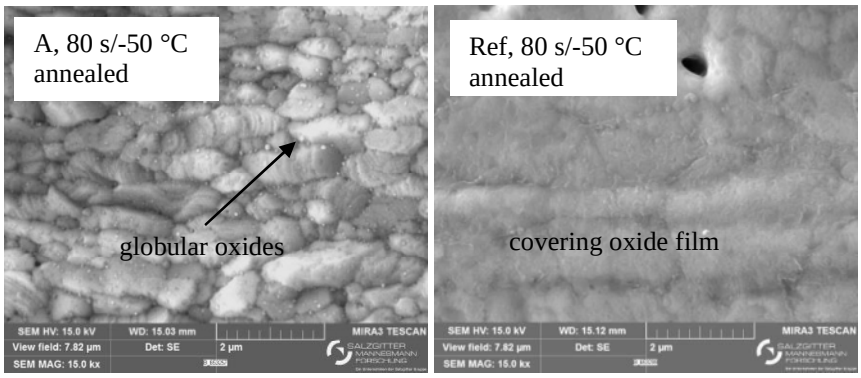

Fig. 8: SEM images from external oxide formation on A and Ref samples with dewpoint -50 °C and short annealing time.

Samples A exhibit less external oxidation after annealing compared to reference samples for the same dew point as can be verified by GDOES depth profiles, see Fig. 9. At dew point -50 °C the surface enrichment for silicon is very high. This can be attributed to a film-like Si rich oxide on the surface which is well known to be detrimental for zinc wetting [1, 2 ,12]. At dew point -30 °C a Cr-enrichment is apparent on the surface, as already seen by Dubois et al. on a Cr-alloyed DP980 [13].

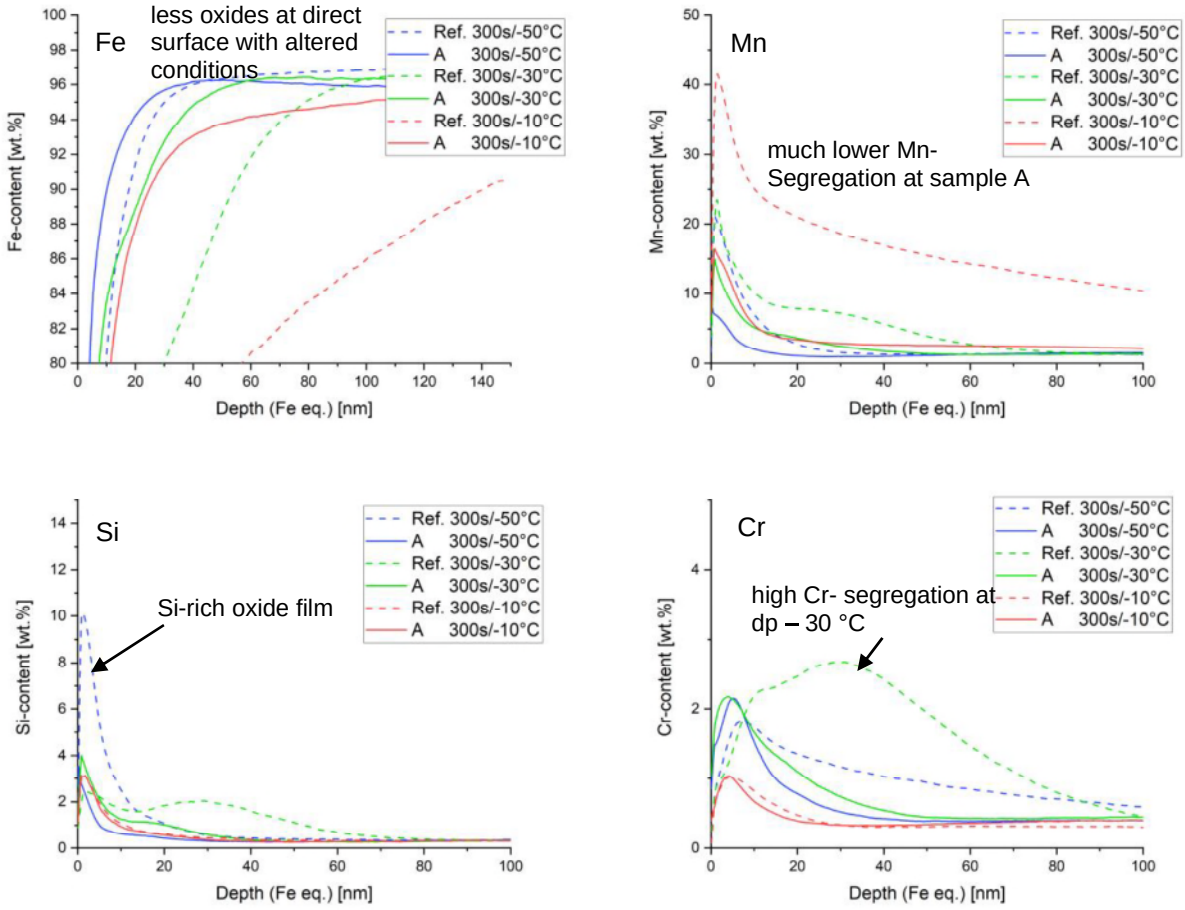

Fig. 9: GDOES depth profiles for Fe, Mn, Si and Cr of altered and reference samples after annealing with dew points of -50°C, -30 °C or -10 °C for 300 s at 850 °C.

Fig. 10 shows the GDOES depth profiles for manganese in comparison before and after annealing step. The depth profiles clearly confirm the segregation of Mn to the surface during the annealing process in both samples. The enrichment at the surface is less pronounced in the altered samples, as the unannealed starting material already shows a deeper Mn-depletion in the surface near region.

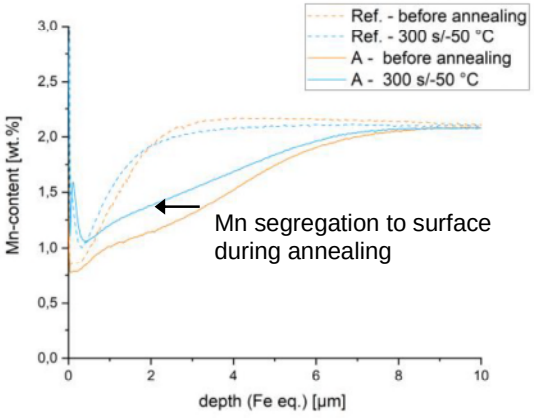

Fig. 10: GDOES depth profiles for Manganese of altered and reference samples before (orange) and after (blue) the annealing step with dewpoint -50 °C.

These differences in external selective oxidation between altered and reference states also influence the galvanising reaction in terms of inhibition layer formation, see Fig. 11. For the same dew point, the altered samples always exhibit a more dense $Fe_2Al_5Zn_x$ layer.

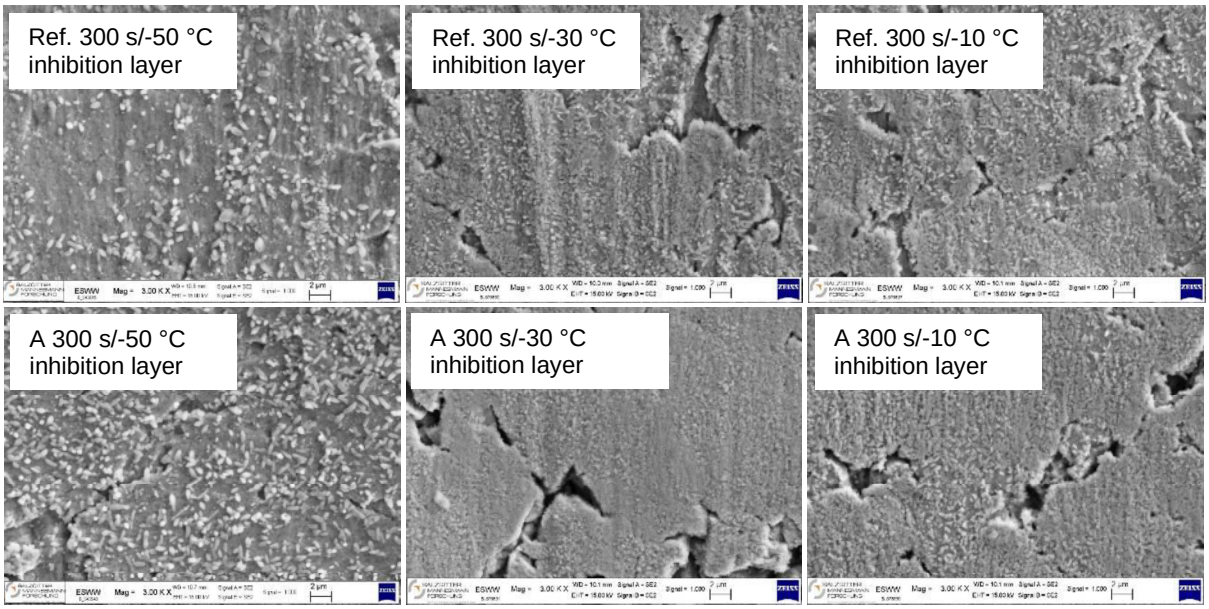

Fig. 11: SEM images of inhibition layer with long annealing cycle for different dewpoints and sample positions.

In addition, small uncoated spots are observed on the reference samples for longer annealing times and dew point -50 °C, which are not present on the -50 °C A samples, see Fig. 12.

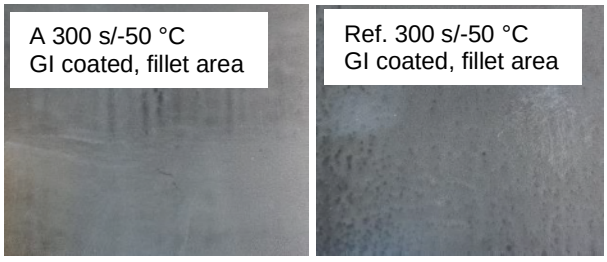

Fig. 12: Macrographs of GI coated samples with long annealing cycle at dewpoint -50 °C.

Adhesion is good for all samples with higher dew points of -30 and -10 °C in 80 and 300 s annealing cycles, see table 1. In dry atmosphere (dew point -50 °C) zinc adhesion decreases significantly as expected. Sufficient zinc adhesion in dry atmosphere can only be observed at short annealing times for A samples.

Table 1: Coating adhesion test results (SEP1931-rating: 1-2 = OK, 3-4 = failure).

Sample	Annealing time	ball impact test (SEP1931)			glue bead test (AA-0509)		
		DP -50 °C	DP -30 °C	DP -10 °C	DP -50 °C	DP -30 °C	DP -10 °C
Ref	80 s	4	1	1	failure	OK	OK
A	80 s	2	1	1	OK	OK	OK
Ref	300 s	4	1	2	failure	OK	OK
A	300 s	4	1	1	failure	OK	OK

This can be explained by the difference in external oxide formation between these samples. At the surface of A, 80 s/-50 °C discrete globular oxides are formed instead of an oxide film, because of the changed µ-topography and the already described depletion zone (see Fig. 9).

3. CONCLUSIONS

The investigations reveal a clear influence of internal oxidation in the coiled state after hot rolling on the galvanisability of high-strength steels. The processes described after hot rolling are summarised and shown schematically in Fig. 13.

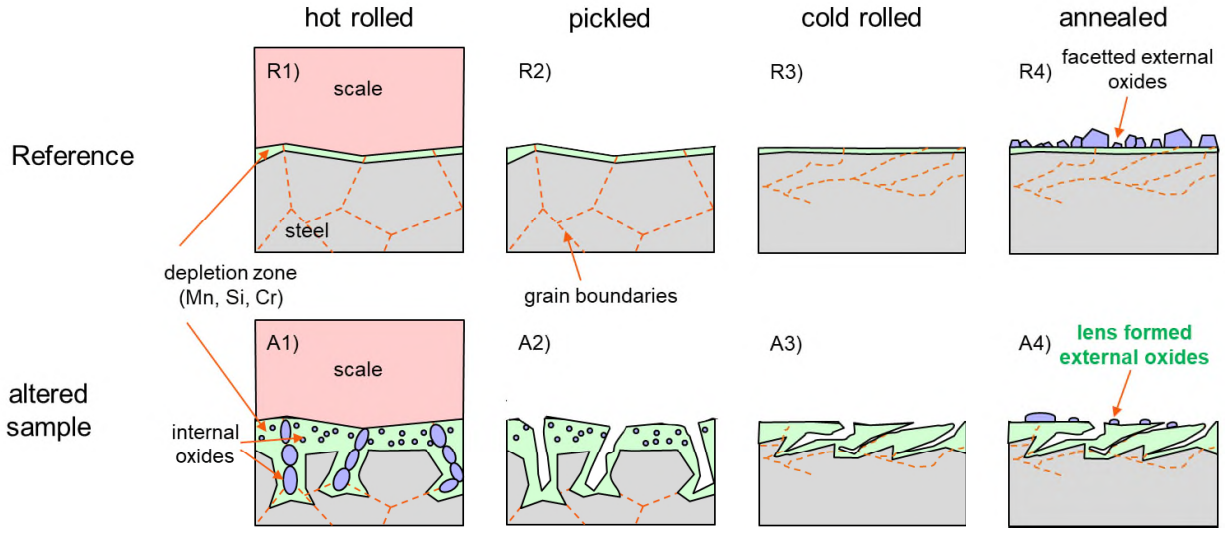

Fig. 13: Schematic diagram on influence of internal oxidation after hot rolling on the subsequent processes and galvanising behaviour (orange: grain boundaries, green: depleted region, blue: oxidised alloying elements, red: scale, grey: steel).

In the FeMnCrSi steel investigated here, a significant internal oxidation of the alloying elements in the volume and especially along the grain boundaries was observed in the centre of the coil under oxygen shortage conditions during cooling of the coiled hot rolled strip (Fig. 13, altered samples, A1). The oxides of the alloying elements at the grain boundaries are hereafter removed selectively in the subsequent pickling process (Fig. 13, A2), which remains visible even after cold rolling. The cold-rolled material with pickled grain boundaries thus shows a changed µ-topography of the surface and, due to the removal of the oxides from the grain boundaries, a measurable depletion of the alloying elements Mn and Cr in the near-surface region of the steel (Fig. 13, A3). During annealing, prior to hot dip galvanising, surfaces with altered µ-topography show reduced surface segregation of alloying elements and therefore less external oxidation (Fig. 13, A4). This results in higher reactivity during hot-dip galvanising under identical annealing conditions and can positively influence coating adhesion.

With sufficient oxygen ingress and high cooling rate after coiling the hot rolled strip, no change in µ-topography of the cold rolled surface was observed (Fig. 13, reference samples, R1-R4).

The described effect could be potentially helpful to enhance galvanisability of future difficult steel grades.

REFERENCES

1) C. R. SHASTRY, J. A. ROTOLE and T. W. KAISER, Galvatech Conf. Proc. (2007), p. 403.
2) Y. SUZUKI, T. YAMASHITA, Y. SUGIMOTO, S. FUJITA and S. YAMAGUCHI, Mat. Sci. Technol., (2009), p. 901.
3) P. DRILLET, Z. ZERMOUT, D. BOULEAU, J.M. MATAIGNE and S. CLAESSENS, Galvatech Conf. Proc. (2004), p. 1123.
4) R. SAGL, A. JAROSIK, G. ANGELI, T. HAUNSCHMIED, G. HESSER and D. STIFTER, Acta Materialia 72, (2014), p. 192.
5) M. AUINGER, V.G. PRAIG, B. LINDER and H. DANNINGER, Corros. Sci. 96, (2015), p.133.
6) L.A. RONQUETI, J. FAVERGEON, M. RISBET and M. PICARD, ABM-Week, Rio de Janeiro, 53rd Rolling Seminar 53 (2016), p. 283.
7) R.Y. CHEN and W.Y.D. YUEN, Oxidation of Met. 56, (2001), p. 89.
8) M.J.L GINES, G.J. BENITEZ, T. PEREZ, E. MERLI, M.A. FIRPO and W. EGLI, Latin Am. Appl. Res. 32, (2002), p. 281.
9) T. FUKAGAWA, H. OKADA, Y. MAEHARA, ISIJ Int. 34, (1994), No. 11, p. 906.
10) L.A. RONQUETI, M. PICARD, J.M. MATAIGNE, J. FAVREGON and M. RISBET, OXI 2018 Eur. Oxide Scale Conf., London, (2018), p. 1.
11) Y. SUZUKI, T. YAMASHITA, Y. SUGIMOTO, S. FUJITA and S. YAMAGUCHI, ISIJ Int. 49, (2009), No.4, p. 564.
12) G. SEYED MOUSAVI and J.R. MCDERMID, Met. & Mat. Trans A 49A, (2018), p. 5546.
13) M. DUBOIS and L. BORDIGNON, AISTTech 2018 Proc., Philadelphia, Pennsylvania (2018), p. 2201.
14) Y. SUZUKI, Y. SUGIMOTO, S. FUJITA, Tetsu-to-Hagané 93, (2007), No. 7, p. 489.
15) H.Y ZHANG, X.-J. LIU, C. WANG, G. ZHOU, L.-J. CHEN, Mater. Res. Express, 6 (2019) 066571.
16) R.Y. CHEN and W.Y.D. YUEN, ISIJ International, 45, No. 1 (2005), p. 52.